

Future Directions of Injectable Hydrogels

Research on injectable hydrogels and related fields is in progress at various top research institutes around the world, and will certainly continue to expand. The key research advances to look for in the future are the development of materials with improved curative efficacy, convenience, and absence of side effects when applied to humans. These developments can be expected to proceed hand in hand with a focus on disease cures, life extension, and investigation of basic life phenomena. Improved understanding of the structural properties of injectable hydrogels that contribute to biocompatibility and therapeutic efficacy, as well as the design and development of original synthesis technology, will facilitate these efforts. At this time, a concerted research effort by workers in various fields is urgently needed to develop and apply original technologies that might help to realize the tremendous potential of injectable hydrogels.

Cross-References

- ▶ [Biomimetics](#)
- ▶ [Self-assembly](#)
- ▶ [Smart Hydrogels](#)
- ▶ [Sol-gel Method](#)

References

1. Temming, K., Fretz, M.M., Kok, R.J.: Organ- and cell-type specific delivery of kinase inhibitors: a novel approach in the development of targeted drugs. *Curr. Mol. Pharmacol.* **1**, 1–12 (2008)
2. Yu, L., Ding, J.: Injectable hydrogels as unique biomedical materials. *Chem. Soc. Rev.* **37**, 1473–1481 (2008)
3. Ruel-Gariépy, E., Leroux, J.C.: In situ-forming hydrogels—review of temperature-sensitive systems. *Eur. J. Pharm. Biopharm.* **58**, 409–426 (2004)
4. Kabanov, A.V., Alakhov, V.Y.: Pluronic block copolymers in drug delivery: from micellar nanocontainers to biological response modifiers. *Crit. Rev. Ther. Drug Carrier Syst.* **19**, 1–72 (2002)
5. Jeong, B., Bae, Y.H., Lee, D.S., Kim, S.W.: Biodegradable block copolymers as injectable drug-delivery systems. *Nature* **388**, 860–862 (1997)
6. Edlund, U., Albertsson, A.C.: Polyesters based on diacid monomers. *Adv. Drug Deliv. Rev.* **55**, 585–609 (2003)
7. Lakshmi, S., Katti, D.S., Laurencin, C.T.: Biodegradable polyphosphazenes for drug delivery applications. *Adv. Drug Deliv. Rev.* **55**, 467–482 (2003)

Injectable In Situ-Forming Gel

- ▶ [Injectable Hydrogel](#)

Insect Flight and Micro Air Vehicles (MAVs)

Hiroto Tanaka¹, Benjamin M. Finio¹, Michael Karpelson¹, Néstor O. Pérez-Arancibia¹, Pratheev S. Sreetharan¹, John P. Whitney¹ and Robert J. Wood²

¹School of Engineering and Applied Sciences, Harvard University, Cambridge, MA, USA

²School of Engineering and Applied Sciences, Wyss Institute for Biologically Inspired Engineering, Harvard University, Cambridge, MA, USA

Synonyms

[Flapping-wing flight](#); [Micro air vehicles \(MAVs\)](#); [Robotic insects](#)

Definition

Micro air vehicles are generally considered to be blown 15 cm in characteristic dimension and weigh on the order of 10 g. Small MAVs, vehicles 1 g or less, have historically relied on insect flight for inspiration and have utilized a variety of flapping-wing morphologies.

This entry discusses sub-gram MAVs inspired by flying insects.

Introduction

Many insect species are agile fliers. Yet they operate in a way fundamentally different from man-made aircraft. Although there are many, sometimes subtle, differences between the flight apparatus of individual species, in general, insects have one or two pairs of wings, driven in multiple rotational degrees of freedom by flight musculature, and powered by metabolic processes which convert chemical energy for flight. Engineers striving to produce a robotic insect must

solve similar challenges, not only for the tasks which the device could perform, but also for the open scientific questions one could use such a device to answer. Therefore, a key question is: how can one manufacture an effective replica of a flying insect? This entry describes the reproduction of some of the key functionalities of a flying insect not as an end “design,” but to prove the viability of the core technologies necessary for such a robot.

The integrated circuit revolution of the 1950s and 1960s now enables the majority of the consumer electronics that are enjoyed daily. As these techniques evolved in the 1980s to include electromechanical components, an even greater space of applications emerged including sensors, optics, and even actuation [1]. Microrobots have been made using MEMS (microelectromechanical systems) surface and bulk micromachining techniques [2, 3]. However, there are many drawbacks to use integrated circuit (IC) and MEMS technologies to create robotic insects. First is the dramatic difference between the material properties of silicon and insect tissue: the former being rigid and brittle while the latter exhibits a large range of material properties, is generally quite resilient, and is approximately the density of water. Second, although the suite of techniques for high resolution machining is an appealing aspect of MEMS processes, the resulting structures are typically “2.5D,” with high aspect ratio components being extremely challenging in terms of machining or requiring hinged structures [4]. Finally, although MEMS foundries exist (e.g., the Multi-User MEMS Process, www.memscapinc.com), cost and turnaround time are generally prohibitive to rapid prototyping. With the advent of “mesoscopic” manufacturing methods [5], researchers have demonstrated key components of the flight apparatus of robotic insects [6] and recently, the first demonstration of a 60 mg flapping-wing device which can produce thrust greater than its body weight [7] has proven the feasibility of creating insect-scale flying robots.

This entry discusses the challenges in developing the components necessary to achieve stable flight of a robotic insect. Topics include aeromechanics, fabrication, actuation, design, control, and power. This entry mostly considers the physical instantiation of a robotic insect. There are numerous additional aspects of a robotic insect that would be required in order for the device to perform useful tasks in natural

environments. These topics will be outlined in the conclusion.

Overview of a Robotic Insect: “RoboBees”

The “RoboBee” project is aiming to build a two-wing robotic flying insect for a variety of tasks including search and rescue and assisted agriculture (e.g., pollination). This section describes the state of the art for the physical instantiation of a robotic bee which consists of composite-reinforced airfoils, a flexure-based transmission, piezoelectric actuation, and a rigid composite airframe. Key to the success of any flapping-wing design is an understanding of the aerodynamics for vehicles of this type and scale; this is discussed in section “[Aerodynamics of Flapping-Wings at Low Reynolds Numbers.](#)”

Aeromechanical Components of a RoboBee

The current RoboBee prototype has four primary mechanical components: thorax, airframe, bimorph piezoelectric actuator, and a pair of airfoils [7], as shown in [Fig. 1a, b](#). To fabricate this bee-sized robot, flexure-based structures are utilized in place of more traditional revolute bearings. A single bending actuator pushes and pulls the upper part of the mechanical thorax in a similar configuration to Dipteran dorsoventral muscles ([Fig. 1c, d](#)). This bioinspired flexure-based transmission is capable of converting small (hundreds of microns – limited by the motion of the piezoelectric actuator) actuator motions into large flapping angles (over 100° peak-to-peak) with a minimum of moving parts and with feature sizes appropriate to the scale of a bee and with extremely high transmission efficiencies. This is otherwise rather difficult, if not impossible, to achieve with a conventional crank mechanism using a rotational motor, rotational bearings, and gears due to part size, assembly accuracy, and friction. The flexure-based structure was utilized not only for transmission hinges but also for precise fabrication and assembly of micro parts. Rigid carbon fiber frames connected with the flexure hinges were fabricated in a plane and then assembled into 3D shapes by folding. This enables precise fabrication and assembly without limiting the materials that can be utilized in the structures. The fabrication process for the flexure-based components is illustrated in [Fig. 2](#). Rigid face sheets are laser

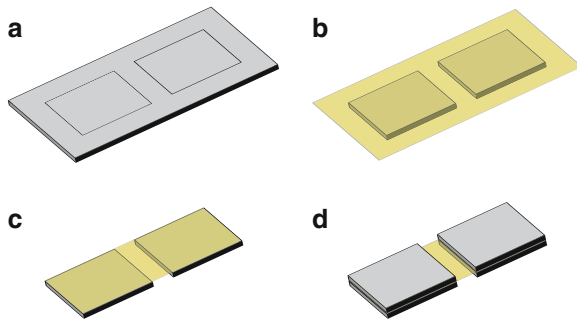
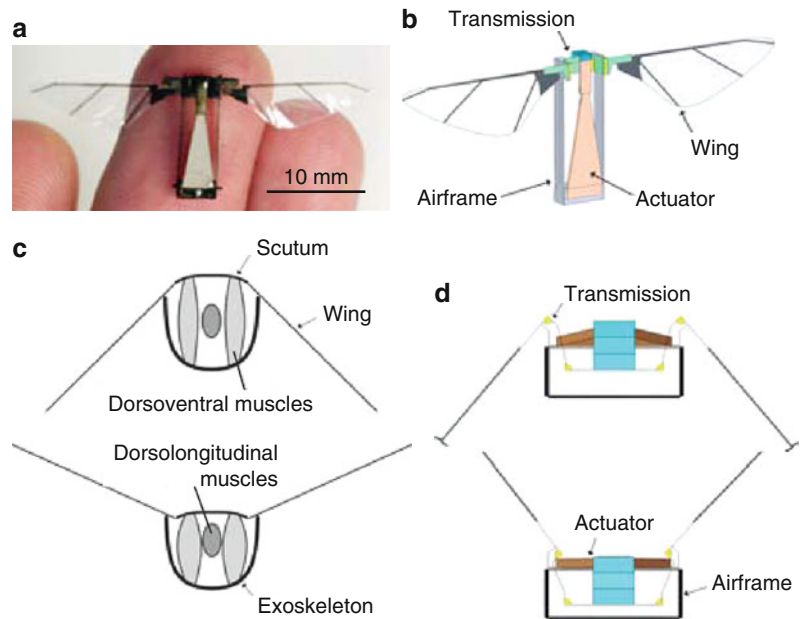
Insect Flight and Micro Air Vehicles (MAVs),

Fig. 1 (a) A prototype RoboBee illustrating scale.

(b) Schematic of the components of RoboBee.

(c) Cross-sectional schematic of Dipteran thorax.

(d) Mechanical thorax of a RoboBee



Insect Flight and Micro Air Vehicles (MAVs),
Fig. 2 Fabrication process for flexure-based articulated structures consisting of carbon fiber rigid plates and a polyimide hinge. First, composite face sheets are laser machined (a) and laminated with a polyimide film (b). This film is laser cut (c) and the structure is laminated to a second face sheet (d)

micromachined using a diode-pumped solid-state laser from carbon fiber reinforced prepreps (preimpregnated with a catalyzed but uncured resin) with precisions and features sizes on the order of $10\ \mu\text{m}$. Thin sheets of polyimide – chosen for mechanical resilience and thermal stability – are also laser micromachined and laminated to the uncured prepreg face sheet using a vacuum tool to ensure uniform pressure distribution. The process is repeated for the opposite face sheet. Airfoils can also be created in this manner but without the need for face sheets on either side of a thin film

polymer membrane. Previous versions have relied on passive flexure hinges at the base of the wing to give rise to the second degree of freedom of the wings: pronation and supination (collectively termed wing rotation). Using these techniques, prototypes as small as 60 mg (15 mm wing length) have been demonstrated [7]. Although all power electronics reside off-board the robot, this device achieved liftoff with vertical rails at a wingbeat frequency of 110 Hz.

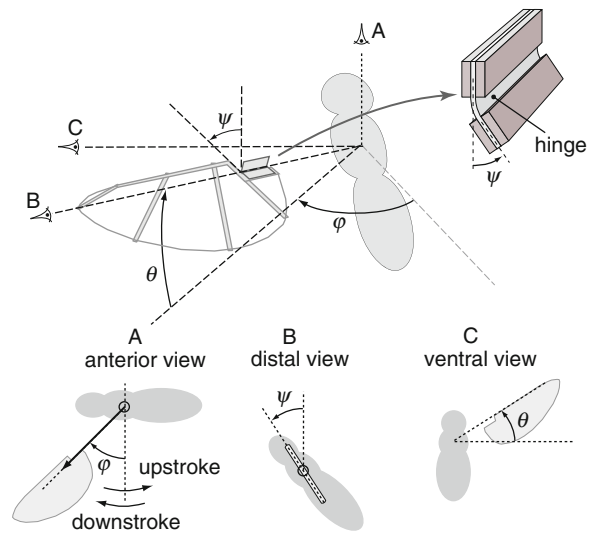
Aerodynamics of Flapping-Wings at Low Reynolds Numbers

Flight at small scales is challenging not only in the development of the mechanism to move the airfoils, but also in the scale-dependent energetic cost of manipulating the fluid. At the scale of insects, with typical Reynolds numbers in the range of 100–10,000 [8], fluid mechanics can be dominated by viscous effects and laminar flow. For example, given a 10 mm long, 5 mm average chord wing operating in air at a 100 Hz flapping frequency with 90° stroke amplitude is operating at an average Reynolds number of approximately 500. In steady flight, these low Reynolds number conditions can dramatically reduce lift-to-drag ratios compared to larger scales and higher velocities. Therefore, there has been significant interest in the study of the “unsteady” mechanisms that insect use to enhance lift production [9].

Flapping kinematics are characterized by large angles of attack at midstroke and high rates of rotation during supination and pronation of the wing. Massive separation of boundary layers, possible reattachment, and strong vortex shedding at both the leading and trailing edges are possible features of this type of flow. In hover, the wing interacts with its own wake, potentially leading to significant time-dependent aerodynamic forces. Needless to say, the wing dynamics and aerodynamic effects involved are complex and the accurate prediction or measurement of forces and flow fields demands sophisticated flow simulations and precise experiments.

Many different aerodynamic effects have been identified, which are reviewed in [10]. Often, experiments attempt to explain the aerodynamics for a single wing at a single operating point, usually with the aim of identifying the important aerodynamic mechanisms for a particular insect species. Recent work by Lentink and Dickinson [11] reverses this trend; they investigate aerodynamic performance under the systematic variation of wing aspect ratio, Reynolds number (Re) and flapping amplitude using a scaled-model mechanical flapping device. As interest in flapping-wing MAVs rises, the study of flapping flight from a design, rather than biological perspective, becomes more important. Instead of studying the behavior and performance of a particular species, research must uncover the important parameters in wing configuration and flapping kinematics that most strongly influence vehicle-level performance for a range of mission profiles and vehicle sizes.

The wing design of a hovering MAV entails not only the capacity for lift generation, but, more importantly, the power required for flight. Hovering is extremely energy-intensive and aerodynamic efficiency is a primary concern. Of equal concern is minimizing the total vehicle mass. Simplification of the wing flapping mechanism and reducing the number of actuated degrees of freedom can lead to great weight savings. To this end, a successful configuration has been developed, where each wing is driven in a single flapping degree of freedom, $\phi(t)$, allowing wing rotation to happen passively. Figure 3 illustrates a wing hinge that allows passive rotation. Clear evidence exists that some insects exhibit passive rotation [12], but there is no consensus that all insects use passive rotation, or that it is necessary for optimal flapping flight. Nevertheless, passive rotation has



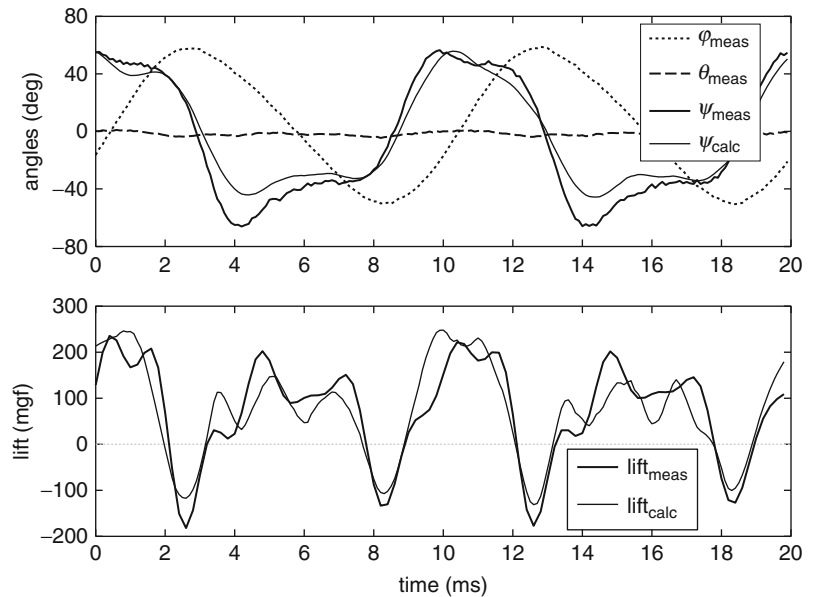
Insect Flight and Micro Air Vehicles (MAVs), Fig. 3 Angles used to specify wing kinematics, shown for a *left* wing and *vertical* body orientation. Current robotic insect prototypes utilize a flexure at the base of the wing (*upper right*) to allow passive rotation. The driving spar (flapping input) mounts to the *top* link of the hinge, the wing to the *bottom*

a demonstrated record of success in flapping-wing MAVs [7]. Prediction of wing performance, in the case of passive rotation, now becomes an aeromechanics problem, as the aerodynamic forces, wing inertia tensor and wing-hinge elastic properties jointly determine the kinematics and resulting forces.

A class of flapping-wing aerodynamic analysis techniques, the so-called blade-element methods are fundamentally a form of dimensional analysis, applied in a careful and systematic fashion. The blade-element method is a quasi-static technique for applying nondimensional experimental and computational results to wings of different scales and operating conditions. The success of this method is critically limited by the quality of the accompanying force and moment coefficients and the method's quasi-static assumptions. The blade-element method begins by dividing the wing into chordwise strips along a flapping wing. The wing must be divided into strips because the relative local velocity varies linearly along the wing. Figure 3 illustrates a wing, flapping in hover, and breaks the kinematics down into flapping (ϕ), out-of-plane deviation (θ) and rotational (ψ) degrees of freedom. Using a simple expression based on dimensional analysis, for the local pressure on the wing, forces and moments arise after a straightforward integration

Insect Flight and Micro Air Vehicles (MAVs),

Fig. 4 Wing kinematics and lift at 100 Hz flapping (Measured and calculated). Measured kinematics are plotted unfiltered



over the entire wing. The key to the blade-element method is experimentally determining the force and moment coefficients, and ensuring that any time-dependence of these coefficients, as a result of unsteady effects, is negligible.

The Reynolds number (Re) for hovering insect flight is typically between 100 and 10,000. This range indicates laminar flow, and a suite of experimental and computational techniques can be employed to predict wing trajectories, deformations, and forces. Scaled-model experiments (e.g., [9]), which mechanically flap scaled-up wings in high-viscosity liquids so as to match Reynolds number, have been very successful in identifying important aerodynamic mechanisms and characterizing the performance of actual insects. However, it is not possible to match the Reynolds number (aerodynamic forces) and the inertial forces simultaneously in a scaled-model experiment. Thus, the scaled-up approaches are not appropriate for studies of passive rotation, or studies of wing deformation. Working with at-scale mechanical flapping mechanisms and micro-force sensors is an experimental challenge, but recent advances in these areas [7, 13] have enabled passive rotation and wing-deformation studies at scale.

The experiment described in [14] consists of a one-axis wing driver mounted to a capacitive force sensor. High-speed video was used to reconstruct the detailed wing trajectory. These kinematics were then

used to generate blade-element force predictions, which could be compared to the experimentally measured forces. Figure 4 illustrates a comparison for one particular wing, flapping at 100 Hz. Hinge stiffness, flapping frequency, and flapping amplitude were varied, and comparisons with blade-element predictions were made for each configuration.

Future work in support of flapping-wing MAV development will focus on continued experimental exploration of the wing design space, with a goal of minimizing the power required to generate the needed lift, under the vehicle mass and manufacturability constraints imposed by the microfabrication technology used, and the power sources available. The design and testing of flexible wings is of particular interest in the continuing quest for higher aerodynamic efficiency.

Toward Autonomy

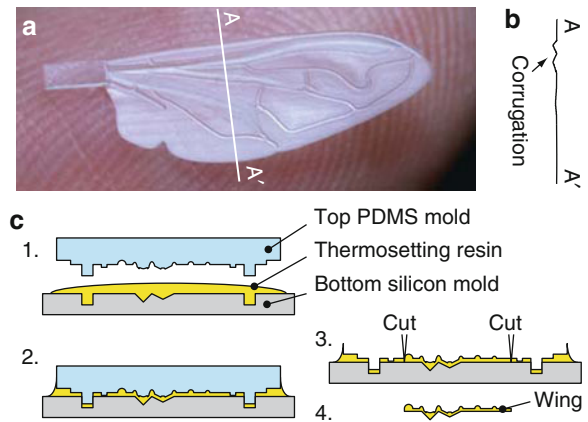
Although a prototype RoboBee achieved takeoff along vertical guide rails, there are myriad challenges which need to be addressed to achieve full autonomy. These topics include, but are not limited to, airfoil design and fabrication, actuation and thoracic mechanics, and control. These topics will be addressed in the following sections.

Biomimetic Flexible Wings

Flexible 3D polymer wings which mimic insect wing morphologies are being developed in addition to the previous rigid carbon fiber based wings described in section “[Aeromechanical Components of a RoboBee.](#)” Real insect wings are flexible and can passively deform when subject to aerodynamic load and inertia force. This flexibility is determined by the wing structure which consists of a thin cuticle membrane supported by a network of tubular cuticle veins [15]. Some insects also have 3D wing profiles such as the corrugation present in Dipteran wings. Actual effects of these wing morphologies on the aerodynamic performance of insect-sized flapping flight, however, are still unknown. By fabricating biomimetic wings, the aim is to develop an understanding of the structure-function relationship for these systems and exploit this understanding to create more effective wings for a robotic insect. Figure 5a shows a fabricated polymer wing mimicking the morphological features of a hoverfly wing [16].

As with a real hoverfly wing, the artificial polymer wings consist of veins with various thicknesses and corrugated profiles (Fig. 5b). Polymer veins and membranes with complex 3D profiles are simultaneously formed by a single molding process with a pair of molds: a bottom rigid (Silicon) mold and a top compliant (PDMS: Polydimethylsiloxane) mold (Fig. 5c). The technical challenge lies in the development of molds with various 3D microscale features: veins, membranes, and corrugation. To realize arbitrary surface profiles in a mold, a custom DPSS (diode-pumped solid-state) laser machining system is used. The surface of a silicon wafer is directly etched with the scanning pulsed laser layer-by-layer to create a 3D negative mold. The spot size of the laser pulse is 10 μm and the etching rate is approximately 5 μm per layer, which is sufficient resolution for the veins and corrugation. The bottom negative mold is directly fabricated with this scanning laser ablation method, and the top PDMS mold is created by casting PDMS on another laser-ablated positive silicon mold.

The thickness of the artificial veins ranges from 50 to 125 μm and the maximum height of the corrugation is 100 μm . Since a hoverfly has vein thickness of 10–70 μm and a maximum corrugation height of 150 μm , this fabrication method enables biomimetic insect wing morphologies in the same scale. The spanwise stiffness of the artificial wing, which



Insect Flight and Micro Air Vehicles (MAVs), Fig. 5
 (a) Photo of an artificial corrugated polymer wing. (b) Measured corrugated profile. (c) Schematic of fabrication process flow

is measured by a point-load bending test, is $2.2 \times 10^{-7} \text{ Nm}^2$. This value has the same order of magnitude of that of *E. dimidiata* (from dried specimens, measured using the same point-load bending test), $5.3 \times 10^{-7} \text{ Nm}^2$, which demonstrates that the artificial wing is statically similar to actual insect wings. These biomimetic wings are useful not only as airfoils for robotic insects, but also for biological studies on insect flight. Unlike experiments with live insects, microfabricated airfoils enable parametric studies of geometric features and experimentally test the relationship between geometry and performance.

Actuators and Thoracic Mechanics

Traditional fixed and rotary wing aircraft use either control surfaces (rudders, ailerons, etc.) or tail rotors to steer. Although insects may use their legs or abdomen to shift their center of mass or aerodynamic profile, their primary steering mechanism is the use of asymmetric wing kinematics [8]. While large, central “power” muscles are responsible for flapping the wings and generating the mechanical power required to stay aloft, in Dipteran insects much smaller “control” muscles at the base of each wing can cause small kinematic changes in wing motion that result in net body torques, allowing the insect to maneuver. A similar approach is used with piezoelectric actuators in the next generation prototype RoboBee (Fig. 6). The wing kinematic parameters, stroke angle ϕ , rotation angle ψ , and deviation angle θ are defined in

Insect Flight and Micro Air Vehicles (MAVs),

Fig. 6 (a) Cross-sectional view (artist's rendering, not anatomically correct) of a Dipteran insect thorax, (b) thorax design with two separate control actuators for changing stroke amplitude, (c) design with a "hybrid" actuator consisting of two bending piezoelectric elements, (d) another hybrid actuator with one bending element and one twisting element. All three designs achieve the same result of differential stroke amplitude

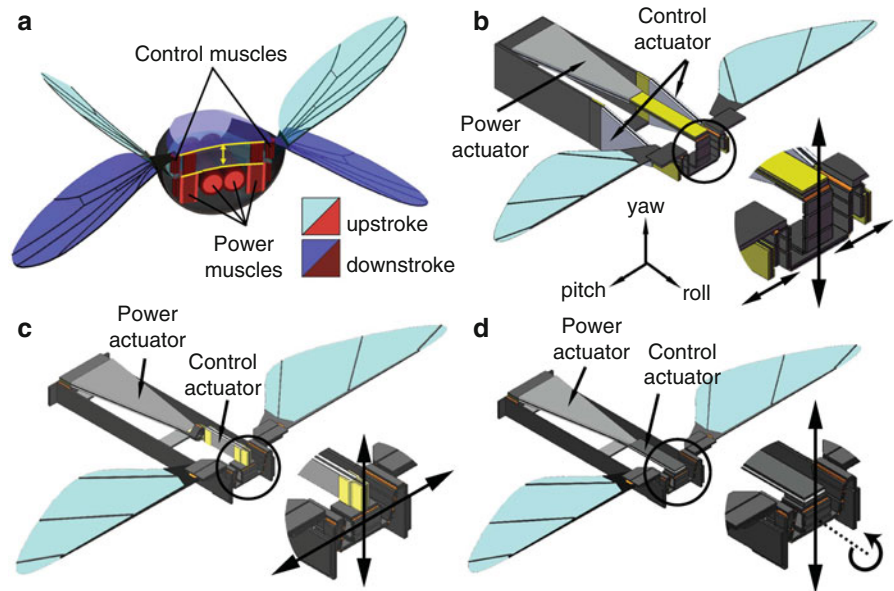


Fig. 3. Since wing dynamics are typically about an order of magnitude faster than body dynamics (i.e., it may take ten wing strokes to complete a 90° turn, although this is not always the case), variation in average parameters over the entire stroke can be sufficient to generate mean body torques. For example (to list only a few possibilities): (a) moving the mean stroke angle for both wings forward of the body's center of mass will result in a pitch torque, (b) differentially increasing the stroke amplitude of one wing to be larger than that of the opposite wing will result in a roll torque, and (c) tilting the stroke plane of one wing forward while tilting the stroke plane of the other wing backward will result in a yaw torque.

Previous prototype RoboBee designs only had one central power actuator, a bending piezoelectric cantilever. Subsequent designs included two smaller control actuators at the base of each wing, allowing controlled stroke amplitude asymmetry [17]. The systems are designed such that very small perturbations to the mechanical transmission connecting the power actuator to the wings by the control actuators can cause large changes in wing trajectory – that is, amplitude differences or stroke-plane deviations on the order of tens of degrees. Several variations of the design for controlled amplitude asymmetry are presented in Fig. 6.

While the ability to modify wing kinematics in a manner similar to that used by Dipteran insects has been verified in [17], actual torque measurements will be required to fully verify aerodynamic models and generate useful feedback control laws for vehicle stabilization and navigation. Work in this area is ongoing.

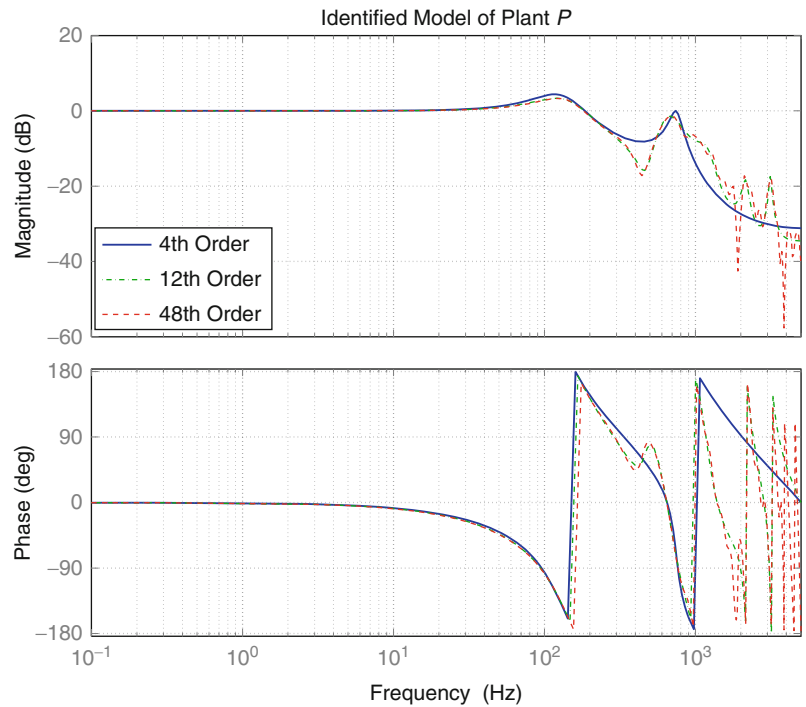
Altitude Control

To date, detailed strategies addressing the problem of altitude control of robotic insects have not been reported. Recent results obtained at the Harvard Microrobotics Laboratory show that by transforming the original problem of altitude control into one of average lift-force control, controllers capable of enforcing specified trajectories along the vertical axis can be synthesized. The main idea is that enough information about the subsystems composing the robotic insect can be gathered a priori, using well-known identification methods, such that, during constrained vertical flight, only an altitude sensor is required.

In this context, there are two subsystems relevant from a control perspective. One is the bimorph actuator, used to transduce electrical into mechanical power, mechanically connected to the insect's airframe. The other is the mapping from the actuator tip displacement to the average lift force generated

Insect Flight and Micro Air Vehicles (MAVs),

Fig. 7 Bode diagram of an identified discrete-time model \hat{P} of the plant P . A 48th-order model is shown in red, reduced 12th and 4th-order models are shown in green and blue, respectively



by the passive rotation of the wings, assuming a sinusoidal excitation of the bimorph actuator. Here, the first subsystem is labeled as P , such that

$$Pu + v = y, \quad (1)$$

where, P is the open-loop dynamics, u is the voltage signal applied to the actuator, y is the output displacement of the actuator tip, and v is an output disturbance signal, representing the aggregated effects of all the disturbances affecting the system, including unmodeled aerodynamic forces produced by the wing flapping.

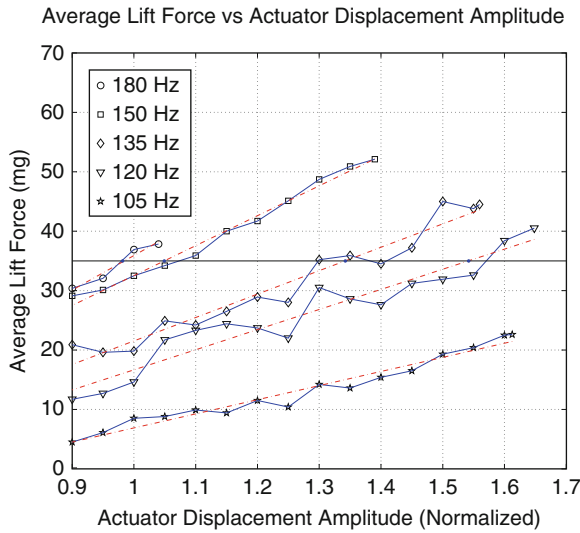
The second subsystem is a static map, labeled as Ψ , such that

$$\Psi(A, f) = \Gamma_L, \quad (2)$$

where, A and f are the amplitude and the frequency of the displacement output $y(t) = A \sin(2\pi ft)$, respectively. The signal Γ_L is the average lift force produced by the flapping of the insect's wings. Typically, instantaneous forces produced by the wings are oscillatory signals with a positive average value. Thus, hovering occurs if Γ_L is approximately equal to the weight of the robotic insect, and vertical motion occurs if Γ_L is

larger than the sum of the insect's weight and the vertical aerodynamic drag. When using digital signal processors for control, Γ_L can be estimated as $\Gamma_L^{(N_L)}(t) = \frac{1}{N_L} \sum_{i=0}^{N_L-1} \gamma_L(kT_s - iT_s)$, where $\gamma_L(t)$ is the instantaneous force measured using a force sensor like the one described in [13], T_s is the sampling time, and $0 < N_L \in \mathbb{Z}^+$, is the number of samples.

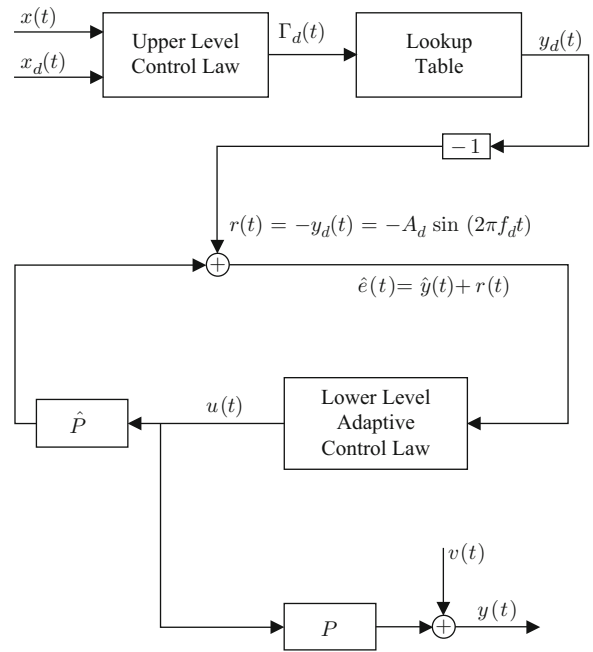
With the use of an appropriate sensor to measure the actuator tip displacement, a discrete-time *linear time-invariant* (LTI) model of P , labeled as \hat{P} , can be found using standard system identification methods. Similarly, with the use of a force sensor, a displacement sensor and a feedback controller capable of enforcing specified trajectories $y(t)$, a lookup table with some relevant points of Ψ can be found through experiments. The estimated mapping \hat{P} and the estimated lookup table associated to Ψ are contingent on a particular microrobotic flapping system, and therefore, great variability should be expected. As examples, in Figs. 7 and 8, an identified model \hat{P} of P , and a graphic representation of an estimated lookup table are shown. These plots were obtained from experiments performed on a single-wing flapping microrobot, similar to the one described in [14]. In Fig. 8, the amplitudes of the



Insect Flight and Micro Air Vehicles (MAVs), Fig. 8 Empirical relationship between lift-force and actuator displacement amplitude, with f taking values of 105, 120, 135, 150, and 180 Hz

signals $y(t)$ are normalized such that a constant input $u(t) = 1$ generates an output equal to 1.

The main idea for designing and implementing controllers is depicted in Fig. 9. Here, the idea is that a desired signal altitude $x_d(t)$ is arbitrarily chosen. Simultaneously, the actual altitude $x(t)$ is measured using an altitude sensor. Both signals are filtered through an *upper level control law* in order to generate a desired average lift-force $\Gamma_d(t)$ which in turn is filtered through an estimated lookup table, like the one graphically shown in Fig. 8, to generate a desired displacement of the actuator tip with the form $y_d(t) = A_d \sin(2\pi f_d t)$. Since A_d and f_d are unknown a priori, the idea of using some type of adaptive cancellation scheme is reasonable. This follows from defining $r(t) = -y_d(t)$ and the error $e_y(t) = y(t) + r(t)$, and then treating $r(t)$ as a disturbance to be rejected. Notice that under the assumption $v(t) = 0$, if $r(t)$ is completely canceled by $y(t)$, the error $e_y(t)$ vanishes and $y(t)$ follows perfectly the desired displacement $y_d(t)$. The other element to be noticed in Fig. 9 is that in order to avoid the need for a displacement sensor during flight, the identified model \hat{P} is used to compute an estimate $\hat{y}(t)$ of $y(t)$, and then, an estimate of the control error, $\hat{e}_y(t) = \hat{y}(t) + r(t)$, is filtered through a *lower level adaptive control law* to generate the control signal $u(t)$ which is the input to the physical system.



Insect Flight and Micro Air Vehicles (MAVs), Fig. 9 Control scheme

To test the proposed method, a single-wing flapping microrobot, similar to the one in [14], is employed in the implementation of hardware-in-the-loop experiments. Since the main idea is to demonstrate lift control using the adaptive scheme in Fig. 9, a simple open-loop upper level control law is used. The objective is to follow an average lift-force signal, $\Gamma_L(t)$, such that a 70-mg robotic insect would move from 0 to 0.3 m and then return to 0 m in no more than 3 s. Using the simple dynamical model of the insect

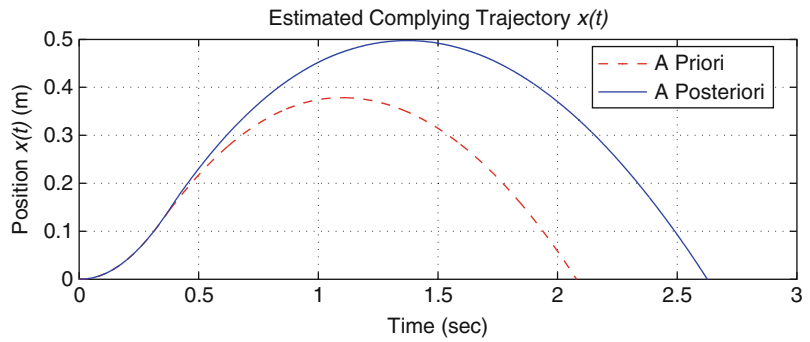
$$\gamma_L - mg = m\ddot{x}, \quad (3)$$

and the experimental data obtained for plotting Fig. 8, through computer simulation the complying a priori trajectory in Fig. 10 was found. Also according to the simulation, the a priori trajectory in Fig. 10 is achievable by tracking the desired lift-force signal in red in Fig. 11, where $N_L = 1,000$.

The resulting experimental average lift force is plotted in blue in Fig. 11, which using the control strategy in Fig. 9, results from choosing $y_d(t) = A_d \sin(2\pi \cdot 150 t)$, with $A_d = 1.2$ for $t \in [0, 0.347]$ s and $A_d = 0.95$ for $t \in [0.347, 5]$ s. The time series of

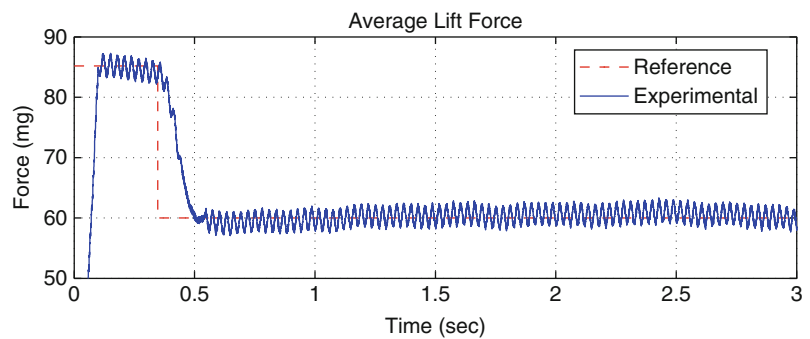
Insect Flight and Micro Air Vehicles (MAVs),

Fig. 10 A priori and a posteriori estimated corresponding trajectories



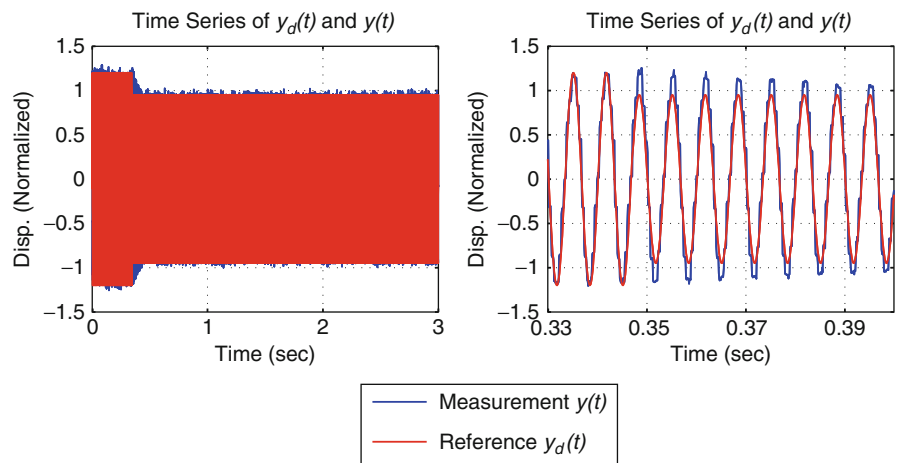
Insect Flight and Micro Air Vehicles (MAVs),

Fig. 11 Reference and experimentally obtained average lift force



Insect Flight and Micro Air Vehicles (MAVs),

Fig. 12 Comparison of time series $y_d(t)$ and $y(t)$ generating the average lift force in Fig. 11. Left Plot: complete series. Right Plot: transition from $A_d = 1.2$ to $A_d = 0.95$



the reference, $y_d(t)$, and output, $y(t)$, are shown in Fig. 12. Here, on the left the complete signals are compared, and on the right the transition from $A_d = 1.2$ to $A_d = 0.95$ is shown. Notice that $y(t)$ is capable of following $y_d(t)$ and that the transition is

smooth, because P is under the control of the feedforward scheme in Fig. 9. According to the hardware-in-the-loop experiments, the estimated resulting *a posteriori* trajectory is shown in blue in Fig. 10.

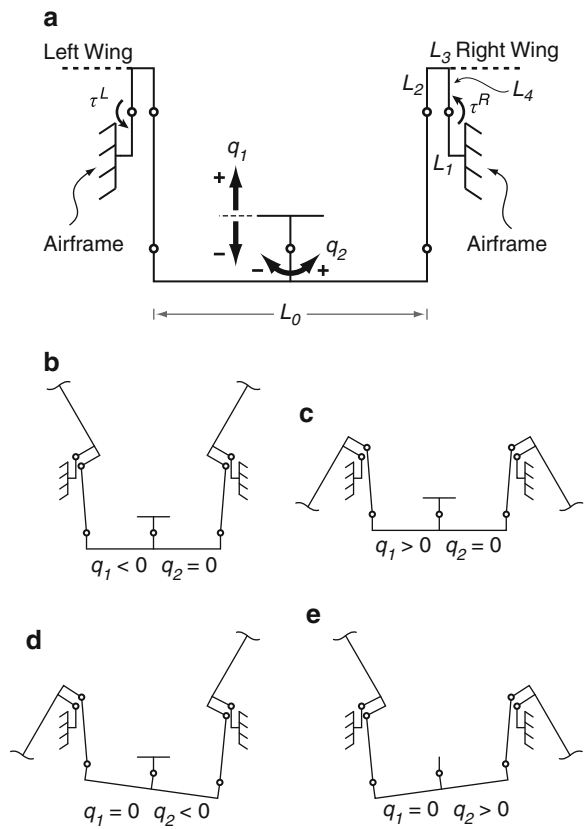
Passive Balancing Transmission

Fully-actuated high-bandwidth control of wing trajectory is a desirable feature for an insect-scale flapping-wing robots and is a conventional approach to attaining control and stability in flight. However, mass and power constraints in such devices motivate the investigation of unconventional control methodologies. A novel methodology, called Passive Aeromechanical Regulation of Imbalanced Torques (PARITY), relies on passive elements to achieve control objectives and has shown much promise in simplifying flight control for a flapping-wing robotic insect.

Passively compliant or under-actuated mechanisms have been used in robotic insects to reduce mechanical complexity, exemplified by the passive hinges allowing the wings of the prototype RoboBee to rotate in flight. The benefits of passive elements, however, can extend beyond reducing mechanical complexity to aid in flight control. The Drag PARITY is an example of such an under-actuated transmission and has been used successfully in the RoboBee to eliminate roll torques imparted to the airframe during operation [18].

Referring to Fig. 13, the Drag PARITY introduces a second degree of freedom to the standard 1DOF RoboBee transmission. Motion along the standard degree of freedom q_1 results in a symmetric flapping motion of the wings, while the additional degree of freedom q_2 allows differential motion between the wings, coupling the upstroke of one wing with the downstroke of the other. This additional degree of freedom is not associated with any actuator; instead, motion along q_2 is determined purely by the dynamics of the system. In this fashion, wing trajectories are passively altered in response to asymmetric wing loading, resulting in a reduction in roll torque experienced by the body of the robot.

Research into PARITY is motivated by the realization that wing trajectories are not of fundamental importance to a flapping-wing device. Ideally, the wings would execute whatever trajectories are necessary to impart the desired forces and torques on the airframe. The fundamental importance of forces and torques over wing kinematics suggests the use of force and torque control instead of kinematic wing control. Passive elements such as those demonstrated by Drag PARITY can alter wing kinematic trajectories on a short timescale in response to forces and torques.



Insect Flight and Micro Air Vehicles (MAVs), Fig. 13

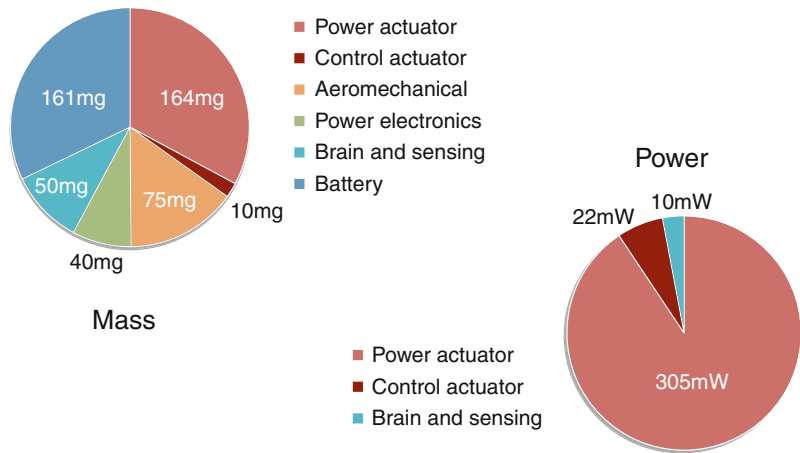
(a) Planar kinematics of the drag PARITY transmission. Holding $q_2 = 0$ and allowing q_1 to oscillate between (b) negative and (c) positive values produces a symmetric flapping motion. Holding $q_1 = 0$ and allowing q_2 to take (d) negative and (e) positive values produces a differential flapping motion, coupling the upstroke of one wing with the downstroke of the other

In this manner, PARITY enabled devices are expected to lower performance requirements on mass and power limited active controllers.

In a PARITY system, active control is achieved not by altering the wing trajectories directly, but by modulating the dynamics of the short timescale passive systems. For example, instead of balancing roll torques, an active control input could bias the system to attain a 10% higher reaction torque from one wing as compared to the other. It is anticipated that enabling such direct control over realized forces and torques will greatly simplify the control problem for mass-limited flapping-wing aeromechanical platforms.

Insect Flight and Micro Air Vehicles (MAVs),

Fig. 14 Mass and power budgets for a hypothetical 500 mg robot

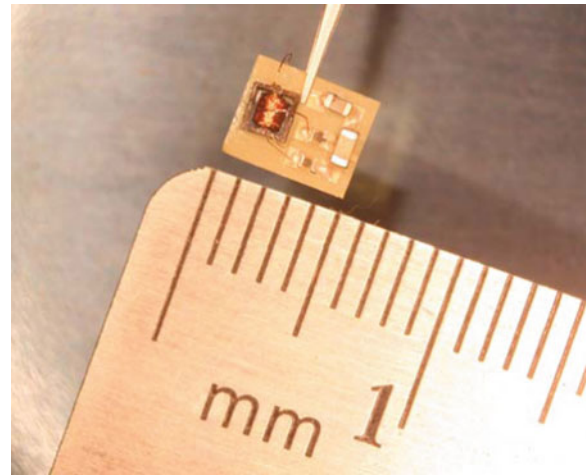


Power Considerations

Power is a key challenge in achieving autonomous operation for insect-sized flapping-wing robots. The stringent weight and power requirements of insect-scale flight, especially when hovering, make it difficult to achieve autonomous operation without a thorough understanding of the interactions and tradeoffs between various components. There are three primary subsystems involved in flight energetics: the aerodynamic components (wings), the power actuators, and the energy source. These subsystems are linked by two transduction mechanisms: the mechanical transmission, which serves as the interface between the actuator and the aerodynamic components, and the power electronics, which serve as the interface between the energy source and the actuator. The remaining subsystems may include: structural, control electronics, sensing, communications, and energy harvesting components.

In the study of power and flight energetics, all subsystems except for the aerodynamic components, the power actuators, and the energy source are classified as payload. Payload is divided into two categories: static payload, which has a fixed mass, and proportional payload, where the mass scales as a percentage of the total mass of the robot.

Continuing advances in the design and characterization of the various subsystems have enabled system-level models of power and energy. The benefits of system-level modeling include analysis of design tradeoffs, optimization for various performance metrics (e.g., flight time), comparison to biological insects



Insect Flight and Micro Air Vehicles (MAVs), **Fig. 15** Twenty milligram voltage converter capable of stepping up a 3.7 V Li-poly battery to 200 V at 70 mW with external control functionality. The converter uses an 8 mg custom laser-micromachined flyback transformer

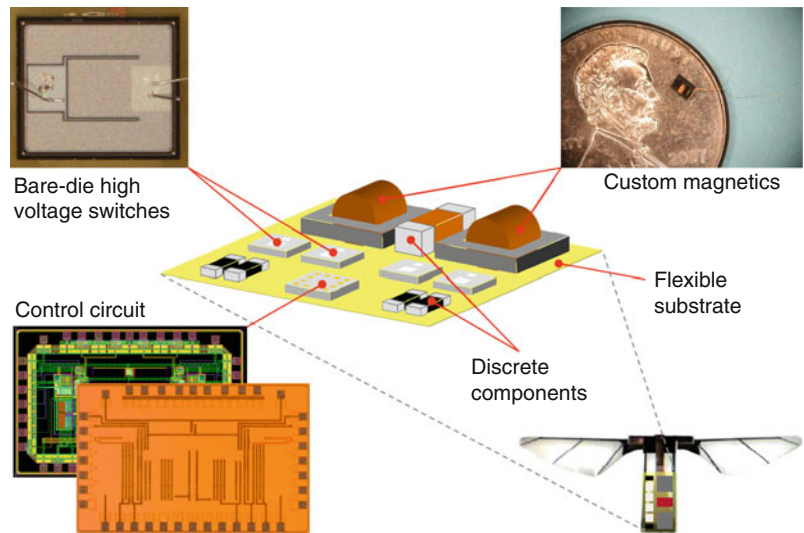
and other aerial platforms, and the ability to estimate the mass and power consumption of system components throughout the design space. For example, Fig. 14 shows the mass and power breakdown for a hypothetical 500 mg (total body mass, with all components integrated) flapping-wing robotic insect, the target vehicle of the RoboBees project [19].

Energy Source

Promising energy sources for robotic insects include batteries, fuel cells, ultracapacitors, and solar cells. At present, lithium polymer batteries are the only

Insect Flight and Micro Air Vehicles (MAVs),

Fig. 16 Power electronics vision



developed, commercially available technology that can satisfy the energy and power requirements of flapping-wing robotic insects. According to the latest models, current battery technology can yield devices that can operate for less than a minute before recharging. A number of new energy storage technologies are currently under development, including micro-solid-oxide fuel cells, lithium batteries with silicon nanowire anodes, and lithium-air batteries. Some of these technologies have the potential to exceed the energy density of current lithium polymer batteries by over an order of magnitude, which will greatly increase the operating time of insect-sized vehicles.

Power Electronics

The wing flapping motion in the RoboBee is powered by piezoelectric actuators, which offer robust mechanical performance, high efficiency, and high-power density at small scales, and are expected to outperform conventional actuators, such as DC motors, in insect-scale devices [6]. From the perspective of power electronic design, piezoelectric actuators present two challenges. Firstly, only a fraction of the input electrical energy is converted to mechanical output, while the remainder is stored in the capacitive structure of the actuator and must be recovered to maximize system efficiency. Secondly, the actuators require high voltages to operate; for example, in the RoboBee, the actuators are driven in the range of

200–300 V. At the same time, prospective energy sources have output voltages below 5 V, while connecting many unit cells in series to obtain high voltage is generally not practical because the packaging overhead causes a significant reduction in energy density.

The power electronics must convert the low input voltage from the energy source into a high-voltage drive signal and recover unused energy from the actuator. Careful selection of switching circuit topologies amenable to miniaturization while retaining high efficiency has enabled milligram-scale step-up voltage converters and drive stages, such as the 20 mg voltage converter in Fig. 15. To minimize weight, the power circuits use a lightweight flexible substrate, chip-scale or bare-die semiconductors, and custom laser-micromachined magnetic components [20].

In order to drive piezoelectric actuators as efficiently as possible, a custom integrated control circuit is used to modulate the high-voltage switches in the power circuits in a way that applies the required drive signal to the actuator terminals while recovering unused electrical energy. The control circuit is manufactured in 130 nm CMOS technology and consumes less than 200 μW , resulting in a negligible effect on system efficiency. The ultimate vision for a milligram-scale power electronics package involves the integration of the power circuits with the control circuit in chip-scale or bare-die form (Fig. 16).

Conclusion

This entry has described enabling technologies for the aeromechanical platform of a flapping-wing robotic insect. This has only focused on the goal of achieving (a) thrust greater than weight, (b) power autonomy, and (c) stable hovering. There are myriad additional topics that need to be addressed in order for these devices to perform useful tasks in natural environments. Sensors for exteroception and proprioception need to be developed and migrated onboard. Low-power computer architectures for flight control and behaviors must reconcile the needs of processing sensory information and calculating actuator responses with the low available power, mass, and volume for anything beyond the flight apparatus. Finally, new methods to program these devices will need to overcome the relative simplicity of the individuals in order to create robust behaviors across a large group of robots.

Beyond the space of applications for insect-like robots, the constituent components are invaluable to help elucidate numerous open scientific questions. Examples include the use of wing fabrication techniques to study the structure-function relationship in natural airfoils and studies of control techniques for under-actuated and computation-limited systems. Various technologies are also motivated by the challenges of robotic insects. Some of these are under development, such as milligram-scale power, low-power computation, novel sensors, and batch meso and microfabrication techniques, while others are more longer-term such as energy harvesting methods.

Acknowledgments This work was supported by the National Science Foundation, the Office of Naval Research, the Army Research Laboratory, the Air Force Office of Scientific Research, and the Wyss Institute for Biologically Inspired Engineering. Any opinions, findings, and conclusions or recommendations expressed in this entry are those of the author and do not necessarily reflect the views of the National Science Foundation.

Cross-References

- ▶ [Basic MEMS Actuators](#)
- ▶ [Biomimetics](#)
- ▶ [Compliant Mechanisms](#)
- ▶ [Nanorobotics](#)

References

1. Petersen, K.: Silicon as a mechanical material. *Proc. of IEEE* **70**, 420–457 (1982)
2. Yeh, R., Kruglick, E., Pister, K.: Surface-micromachined components for articulated microrobots. *J. Microelectr. Mech. Syst.* **5**(1), 10–17 (1996)
3. Donald, B., Levey, C., McGray, C., Paprotny, I., Rus, D.: An untethered, electrostatic, globally controllable mems micro-robot. *J. Microelectr. Mech. Syst.* **15**(1), 1–15 (2006)
4. Pister, K., Judy, M., Burgett, S., Fearing, R.: Microfabricated hinges. *J. Sens. Actuator A Phys.* **33**, 249–256 (1992)
5. Wood, R., Avadhanula, S., Sahai, R., Steltz, E., Fearing, R.: Microrobot design using fiber reinforced composites. *J. Mech. Des.* **130**(5), 052304 (2008)
6. Wood, R.J., Steltz, E., Fearing, R.S.: Optimal energy density piezoelectric bending actuators. *J. Sens. Actuator A Phys.* **119**(2), 476–488 (2005)
7. Wood, R.L.: The first flight of a biologically-inspired at-scale robotic insect. *IEEE Trans. Robot.* **24**(2) (2008)
8. Dudley, R.: *The Biomechanics of Insect Flight: Form, Function, Evolution*. Princeton University Press, Princeton, NJ (2000)
9. Dickinson, M.H., Lehmann, F.-O., Sane, S.P.: Wing rotation and the aerodynamic basis of insect flight. *Science* **284**, 1954–1960 (1999)
10. Sane, S.P.: The aerodynamics of insect flight. *J. Exp. Biol.* **206**(23), 4191–4208 (2003)
11. Lentink, D., Dickinson, M.H.: Rotational accelerations stabilize leading edge vortices on revolving fly wings. *J. Exp. Biol.* **212**(16), 2705–2719 (2009)
12. Ennos, A.R.: The inertial cause of wing rotation in Diptera. *J. Exp. Biol.* **140**, 161–169 (1988)
13. Wood, R.J., Cho, K.-J., Hoffman, K.: A novel multi-axis force sensor for microrobotics applications. *Smart Mater. Struct.* **18**(12), 125002 (2009)
14. Whitney, J.P., Wood, R.J.: Aeromechanics of passive rotation in flapping flight. *J. Fluid Mech.* **660**, 197–220 (2010)
15. Wootton, R.J., Herbert, R.C., Young, P.G., Evans, K.E.: Approaches to the structural modelling of insect wings. *Philos. Trans. R. Soc. Lond. B Biol. Sci.* **358**, 1577–1587 (2003)
16. Tanaka, H., Wood, R.J.: Fabrication of corrugated artificial insect wings using laser micromachined molds. *J. Micromech. Microeng.* **20**, 075008 (2010)
17. Finio, B.M., Wood, R.J.: Distributed power and control actuation in the thoracic mechanics of a robotic insect. *Bioinspir. Biomim.* **5**, 045006 (2010)
18. Sreetharan, P.S., Wood, R.J.: Passive aerodynamic drag balancing in a flapping wing robotic insect. *J. Mech. Des.* **132**(5), 051006–051016 (2010)
19. Karpelson, M., Whitney, J., Wei, G.-Y., Wood, R.: Energetics of flapping-wing robotic insects: towards autonomous hovering flight. In: *Intelligent Robots and Systems (IROS)*, 2010 IEEE/RSJ International Conference on, Taipei, Taiwan, pp. 1630–1637 (2010)
20. Karpelson, M., Whitney, J., Wei, G.-Y., Wood, R.: Design and fabrication of ultralight high-voltage power circuits for flapping-wing robotic insects. In: *Applied Power Electronics Conference and Exposition (APEC)*, 2011 Twenty-Sixth Annual IEEE, Fort Worth, TX (2011)